Science Bulletin 70 (2025) 1445–1451

Contents lists available at ScienceDirect

Science Bulletin

journal homepage: www.elsevier.com/locate/scib

Article

A 300-km fully-connected quantum secure direct communication network

Yilin Yang [a,1], Yuanhua Li [a,b,1,*], Hao Li [a], Chennan Wu [a], Yuanlin Zheng [a,c], Xianfeng Chen [a,c,d,*]

[a] State Key Laboratory of Advanced Optical Communication Systems and Networks, School of Physics and Astronomy, Shanghai Jiao Tong University, Shanghai 200240, China
[b] Department of Physics, Shanghai Key Laboratory of Materials Protection and Advanced Materials in Electric Power, Shanghai University of Electric Power, Shanghai 200090, China
[c] Shanghai Research Center for Quantum Sciences, Shanghai 201315, China
[d] Collaborative Innovation Center of Light Manipulation and Applications, Shandong Normal University, Jinan 250358, China

ARTICLE INFO

Article history:
Received 29 November 2024
Received in revised form 2 January 2025
Accepted 17 February 2025
Available online 27 February 2025

Keywords:
Quantum information
Quantum secure direct communication
Quantum network
Nonlinear optics

ABSTRACT

Transmission distance and number of users limit the realization of large-scale scalable quantum communication networks, as existing quantum network construction techniques struggle to address these two important factors simultaneously. In this paper, we propose a long-distance large-scale and scalable fully-connected quantum secure direct communication (QSDC) network, which employs a double-pumped structure and the introduction of extra noise to successfully realize QSDC over 300 km between four users in the network in pairs. The results demonstrate that the fidelity of the entangled state shared between users following communication remains above 85%. The results of our research demonstrate the viability of this quantum communication network, offering a novel foundation for the future realization of long-distance large-scale quantum communication.

1. Introduction

The quantum network represents a significant platform for the verification of the fundamental principles of quantum mechanics and the realization of quantum communication and computation [1,2]. As point-to-point quantum communication technology matures, the construction of long-distance, large-scale, and scalable quantum communication networks has emerged as a prominent area of research [3–5]. At present, a number of distinct quantum network architectures have been proposed, such as quantum key distribution (QKD) networks [6–9], deterministic quantum networks [10], and entanglement distributed quantum networks [11]. In QKD networks, the inherent limitations of transmission distance and point-to-point communication frequently necessitate the deployment of quantum relaying techniques to enhance transmission distances and expand the quantum state of the network. In deterministic quantum entanglement switching networks, two single-photon sum-frequency techniques are necessary to distinguish between four sets of Bell states. However, the low efficiency of single-photon sum-frequency restricts the transmission distance of the communication network. In entanglement distributed quantum networks, the complexity and noise of single-pump schemes increase with the number of users, thereby limiting the size of the network. The transmission distance or the number of users acts as a constraint on the construction of long-distance, large-scale quantum communication networks, and all three types of schemes are difficult to build. The realization of a 10,000-km-level quantum communication network containing hundreds or thousands of users represents a significant challenge that requires urgent attention. There are three main forms of communication used in quantum networks, which are QKD [12,13], quantum teleportation [14,15], and quantum secure direct communication (QSDC) [16,17]. QKD only shares the key, while quantum teleportation and QSDC can pass the information directly. Since QKD uses approximate single-photon sources or weakly coherent pulsed sources produced by attenuating classical light sources, it is advantageous for communication over thousands of kilometers. On the other hand, for discrete-variable quantum teleportation, it uses a photon-entangled source as a quantum channel to directly transmit information using a single photon as the information carrier [18]. For continuous-variable quantum teleportation, it does not use single photons as carriers and can transmit multiple bits [19]. However, in quantum stealthy communication, a photon can only carry one classical message. The QSDC scheme

* Corresponding authors.
E-mail addresses: lyhua1984@shiep.edu.cn (Y. Li), xfchen@sjtu.edu.cn (X. Chen).
[1] These authors contributed equally to this work.

https://doi.org/10.1016/j.scib.2025.02.038
2095-9273/

was first proposed by Long and Liu [20], which also uses a single photon as an information carrier, but unlike the quantum teleportation scheme, a single photon in QSDC can directly transmit two classical messages. Nowadays, an increasing number of theories and experiments have demonstrated the viability of this scheme [21–29]. In theory, the one-step QSDC [30], device-independent (DI) QSDC [31–33], measurement-device-independent (MDI) QSDC [34,35], the QSDC using hybrid entanglement [24], continuous-variable (CV) QSDC protocols [36], and passive decoy-state QSDC [23] are proposed. In experiments, the first single-photon QSDC entanglement, the first entanglement-based QSDC experiment [37], and the first long-distance fiber QSDC experiment [38] are demonstrated. In addition, some other significant experiments, such as QSDC over 100 km of optical fiber [39] and a 15-user QSDC network over 40 km [40], were also reported. QSDC has emerged as a pivotal technology for the construction of quantum communication networks [41]. Fortunately, we found that multipump technology enables photons of the same wavelength to interact with photons of multiple wavelengths during the preparation of associated photon pairs. This suggests that a fully- connected quantum network constructed using multipump technology can exhibit reduced complexity. In the event of constrained quantum correlation links, the network constructed by multipump technology is capable of accommodating a greater number of users, thereby circumventing the limitation of user capacity. Furthermore, the incorporation of an appropriate degree of additional noise can markedly increase the performance of quantum communication [42–44]. To mitigate the impact of quantum noise on transmission distance, additional noise can be introduced prior to the distribution of photon pairs, thereby compensating for some of the noise and improving the fidelity of shared entangled states between users after transmission, as well as the transmission distance. When these two techniques are employed in the construction of a quantum network, both the number of users and the transmission distance can be enhanced. In this work, we propose a novel long-distance scalable fully-connected QSDC network in noisy environments. In our experiment, we employ a double-pumped structure design and a custom-made on-chip periodically poled lithium niobate (PPLNOI) to generate polarization-entangled photon pairs across multiple quantum correlation links, thereby entangling the four users in the network in pairs. Furthermore, the introduction of additional noise prior to the distribution of photon pairs enables the achievement of QSDC over 300 km of fiber between arbitrary users. The fidelity of the entangled states shared by the users after communication is greater than 85%. Our scheme provides an effective approach to scaling up quantum networks and improving transmission distances, as well as a novel idea for the construction of quantum networks on compact integrated platforms.

2. Experiment

The structure of the large-scale scalable fully-connected QSDC network we have designed is shown in Fig. 1. The quantum processor employs a multitude of pumps with distinct wavelengths to concurrently generate entangled photon pairs, and then utilizes dense wavelength division multiplexing (DWDM) to disseminate the photons of a specific channel to disparate distant users, thereby guaranteeing that the association between any two of them is established by at least one pump. In accordance with this network design scheme, the number of pumps utilized is inversely proportional to the number of channels a user is required to operate. In a fully-connected network comprising N users, the number of pumps, M, ranges from 1 to $2N-3$. When $M=1$, the total number of channels required by the users is at least $2C_N^2$, which is the same as that required by a classical single-pump fully-connected quantum network. When $M=2$, the total number of channels required by the users is at least C_N^2+2 ($N \geqslant 4$), which is nearly halved at larger N. When $M=2N-3$, each user only needs to operate a single channel of photons for QSDC between each other. This indicates that the objective of accommodating a greater number of users in the network and overcoming the limitation of the number of users can be achieved by increasing the number of pumps and consequently reducing the total number of channels required by users. In our experiment, we establish entanglement by distributing polarization-entangled photon pairs. The sender selects different basis vectors for the measurement by performing a Missile transformation on the photons it receives and sends the measurement results to the receiver. The receiver then combines the photon measurements with the Bell-state analysis to obtain the information transmitted by the sender. We will subsequently provide a brief description of the QSDC employed by each user within the network [45]. The polarization entanglement shared between users communicating with each other is represented by $|\varphi^+\rangle = \frac{1}{\sqrt{2}}(|HH\rangle + |VV\rangle)_{\lambda_1(\lambda_2\lambda_3\cdots\lambda_M)}$, where H and V represent horizontal and vertical polarization, respectively, λ_m ($m=1,2,\cdots,M$) represents the wavelength of the pump light. The particular methods of communication are as follows: (1) The security of the quantum channel is verified in pairs between users. Different pumps produce single photons of the same wavelength, but their corresponding associated photons do not have the same wavelength in the limit of energy conservation. We know that only conforming counts measurements of associated photon pairs produce conforming counting peaks at specific event intervals. Since photons generated by spontaneous parametric down-conversion (SPDC) are random, photons of the same wavelength generated by other pumps will be uniformly distributed over different time intervals. In this case, for any two-user communication scenario, only the entangled photons generated by the pumps that make their association are considered signal photons, while all photons produced by other pumps within the user channel are classified as noise photons. To ascertain the security of the quantum channel, the quantum processor orchestrates the sequence of light emitted from the various pumps, thereby separating the positions of the signal photons from those of the noise photons. Subsequently, each user performs a comparison between the positions of the signal and noise photons to determine the safety of the quantum channel. (2) Once the security verification process is complete, each user engages in a four-party negotiation of the four sets of Bell states corresponding to different bit values. For instance, $|\varphi^\pm\rangle_{\lambda_1(\lambda_2\lambda_3\cdots\lambda_M)} = \frac{1}{\sqrt{2}}(|HH\rangle \pm |VV\rangle)_{\lambda_1(\lambda_2\lambda_3\cdots\lambda_M)}$ is associated with 00, 01, while $|\phi^\pm\rangle_{\lambda_1(\lambda_2\lambda_3\cdots\lambda_M)} = \frac{1}{\sqrt{2}}(|HV\rangle \pm |VH\rangle)_{\lambda_1(\lambda_2\lambda_3\cdots\lambda_M)}$ is linked to 10, 11, respectively. (3) When any user U_i wishes to establish communication, he performs operations on the photons (comprising both signal and noise photons) received by himself in the channel. This is done with one of four distinct quantum gates: $I, \sigma_z, \sigma_x, -i\sigma_y$. As a result, the form of the shared polarization entanglement will change to one of the four different quantum states $|\varphi^+\rangle, |\varphi^-\rangle, |\phi^+\rangle, |\phi^-\rangle$, respectively. These four quantum states correspond to the encoding information 00, 01, 10, and 11, respectively. (4) The other communicating user, who shares the entangled state with user U_i, determines the quantum gate selected by user U_i based on the results obtained by performing the Bell-state measurement to obtain the transmitted information. In consideration of the impact of noise, the density matrix of entangled photon pairs shared between any two users, designated as A and B, before transmission is represented by the symbol ρ. In our proposed scheme, we seek to mitigate the impact of noise generation during transmission by introducing an additional noise source. Following the introduction of this additional noise source,

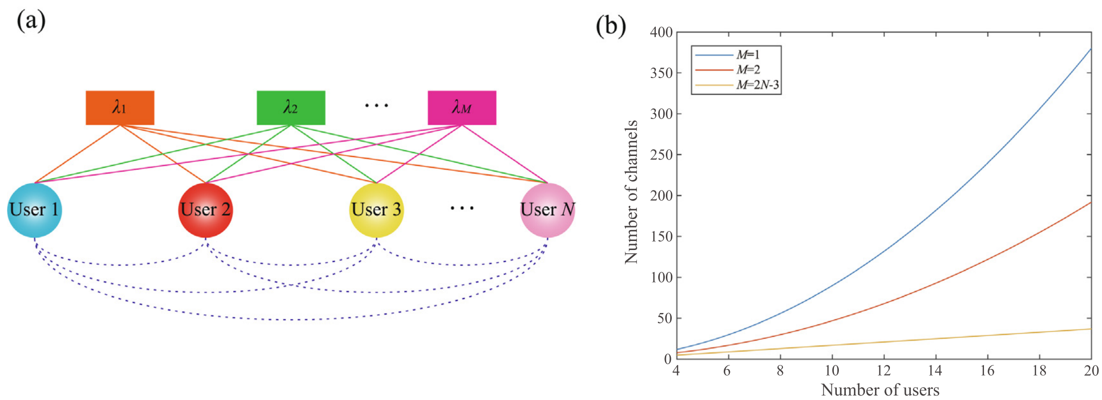

Fig. 1. (a) Conceptual diagram of a large-scale fully-connected QSDC network. (b) Number of channels versus number of users in different number of pumps.

the density matrix of entangled photon pairs after transmission is given by [42]

$$\rho' = \sum_{j=1}^{n_A}\sum_{k=1}^{n_B} E_{jk}(p_A, p_B)\rho E_{jk}^{\dagger}(p_A, p_B), \quad (1)$$

where E_{jk} is the operator which represents a certain type of noise. In this paper, we consider only the bit flip type of noise, so p_A, p_B denote the total probability of inversion of two optical quantum bits. The total probability of bit inversion should contain two portions, i.e. $p_A = p_{A,trans} + p_{A,extra}, p_B = p_{B,trans} + p_{B,extra}$, the portion attributable to the transmission is determined by the quantum channel, whereas the additional portion introduced is adjustable by the additional noise-generating device. The optimal selection of an appropriate noisy environment can markedly enhance the fidelity of entangled photon pairs following transmission. However, in practice, the regulation of the noise environment frequently relies on the photon counting of detectors at the user's end. The advantage of the multipump network structure is that it not only reduces the complexity of the system, but also increases the number of photons in a single channel of the user. This helps to overcome the noise-induced degradation of the fidelity of the entangled photon pairs. Furthermore, as the loss of photons is determined within the C-band fiber channel, the increase in the number of photons within the user's individual channel can also enhance the transmission rate and transmission distance of the information. The particular quantum network optical path utilized in the experiment is illustrated in Fig. 2a. As the temperature-controlled PPLN waveguide is only capable of guaranteeing the efficiency of the second harmonic generation (SHG) of two or three pumps corresponding to the C-band in the International Telecommunication Union (ITU) at a fixed temperature, we present only the construction of a double-pumped fully-connected network, i.e., $M = 2$. Our PPLNOI chip is employed in a polarization Sagnac interferometer to facilitate the generation of polarization-entangled single-photon pairs with the Bell state $|\varphi^+\rangle_{\lambda_1(\lambda_2)} = \frac{1}{\sqrt{2}}(|HH\rangle \pm |VV\rangle)_{\lambda_1(\lambda_2)}$ [46]. These pairs are produced via the SPDC process occurring at temperatures near room temperature, and are characterized by low noise and high quality. Fig. 2b, c illustrate the measurement outcomes for the properties of our PPLNOI waveguide chip. The orange curves represent theoretical calculations, while the blue square dots represent data points obtained from experimental results. The entangled single photon pairs generated by the two pumps are distributed to the four users via a DWDM, ensuring that a set of polarization-entangled photon pairs is shared between the two users. The construction of the QSDC network in our experiment is comprised of three distinct parts: the generation of entangled photon pairs, the distribution and transmission of photon pairs, and the user modulation and detection. In the entangled photon pair generation part, the wavelengths of the two tunable narrowband continuous lasers serving as the laser sources are tuned to 1551.72 nm (CH32) and 1550.92 nm (CH33), respectively. These wavelengths are then amplified with two erbium-doped fiber amplifiers (EDFAs). The amplified pump light is then combined with the other beams in a DWDM and connected to a PPLN for SHG process, which doubles the frequency of the pump light. A wavelength division multiplexing (WDM) with an extinction ratio of 180 dB (S/N: 224851568, Shenzhen Xianyitong Technology Company) is used to suppress the initial light from CH32 and CH33. To maintain the quasi-phase matching condition of the SHG process, two polarization controllers (PCs) are utilized to regulate the polarization of the pump light prior to DWDM beam combining. Additionally, a stabilized temperature controller is employed in the PPLN to maintain the temperature. The temperature of the PPLN in the experiment is set at a point midway between the optimal temperature at the wavelengths of 1551.72 and 1550.92 nm, thereby ensuring a high SHG efficiency for both pump beams. The frequency-doubled pump light is launched via a spatial optical coupler as the transmitter into the polarization Sagnac interferometer to produce polarization-entangled photon pairs, and then are subsequently collected by another spatial optical coupler into a single-mode fiber. In the photon pair distribution and transmission part, the collected single-photon pairs are separated by a 100-GHz DWDM, and different additional noises are applied separately by an additional noise generator. Subsequently, the photons of the CH31 and CH36, CH33 and CH34, CH32 and CH35, and CH29 and CH30 channels are transmitted to users 1–4 via optical fibers, respectively. In the user modulation and detection part, each user is equipped with a polarization state analyzer consisting of a half-wave plate (HWP), a quarter-wave plate (QWP), and a polarization beam splitter (PBS), as well as a superconducting nanowire single-photon detectors (SNSPD) [47,48]. The SNSPD, which is employed to detect photons received by the user, exhibits a detection efficiency exceeding 80% with a dark count rate of 40–100 Hz, and the resulting photon detection data are recorded by a time-to-digital converter (TDC) (ID-900). Each user can perform Bell-state measurement twice by using linear optical elements to determine one of the four Bell states [49].

3. Results

To verify the polarization entanglement characteristics of the fully-connected network, we conducted measurements of the polarization entanglement characteristic curves and fidelity of the correlation channels between each user. The resulting data are presented in Figs. 3 and 4, where the blue data points and

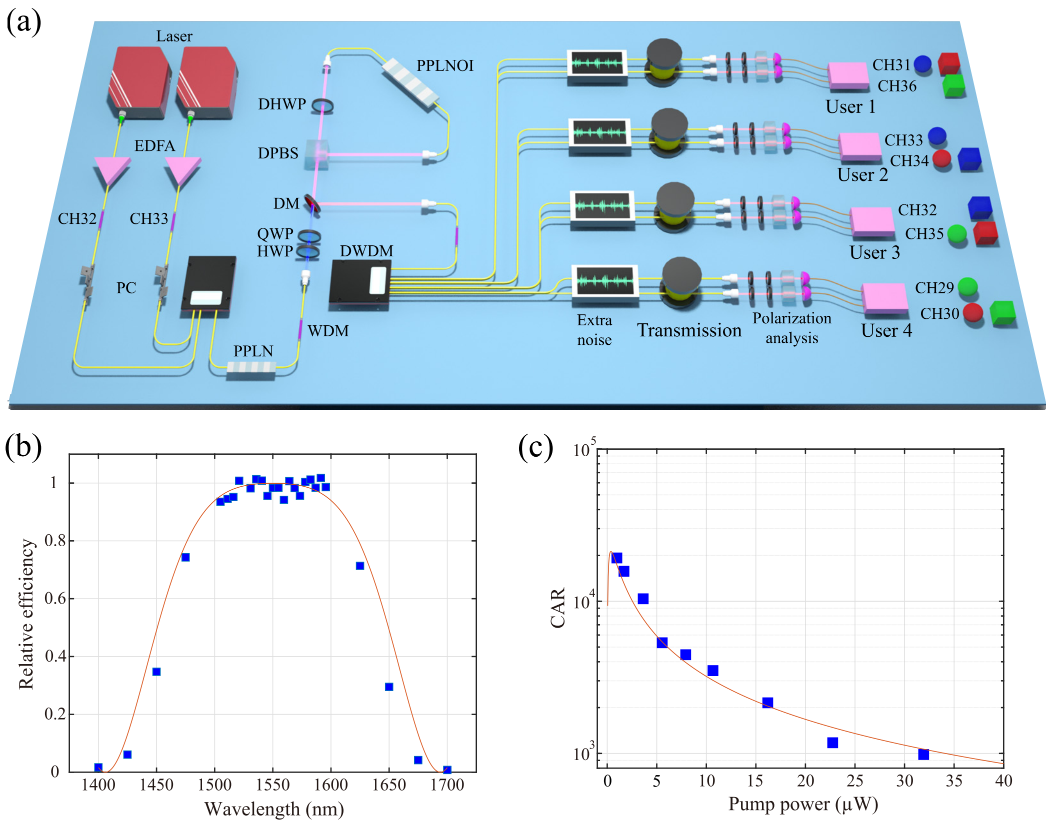

Fig. 2. The experimental setup. (a) The physical structure of the QSDC network comprises the following elements. Laser: narrowband continuous laser; EDFA: erbium-doped fiber amplifier; PC: polarization controller; PPLN: periodically poled lithium niobate; WDM: wavelength division multiplexing; HWP: half-wave plate; QWP: quarter-wave plate; DPBS: dual-wavelength polarization beam splitter; DM: dichroic mirror; DWDM: dense wavelength division multiplexing; PPLN: periodically poled lithium niobate; PPLNOI: on-chip periodically poled lithium niobate. (b) Typical spectrum of the SPDC source based on PPLNOI waveguide. Relative efficiency denotes the conversion efficiency under the spontaneous parameter after normalization. (c) Variation of the coincidence-to-accidental ratio (CAR) of photon pairs generated by the PPLNOI waveguide with pump power.

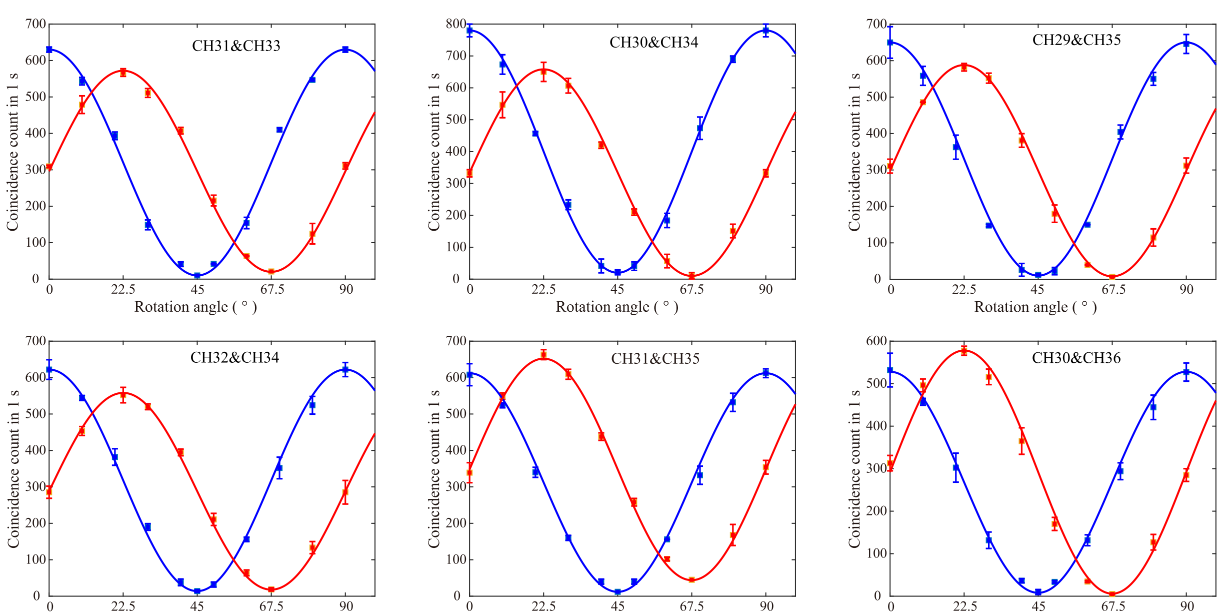

Fig. 3. The characteristic curve of polarization entanglement for each user-associated channel.

the red data points represent the two-photon coincidence count measured by rotating the angle of the other HWP when the angle of one side of the HWP is fixed at 0° and 22.5°, respectively. The detection time for each data point is 1 s, and the results demonstrate that the fidelity of each channel is greater than 97%. In the experiment, we establish a secure quantum entanglement channel

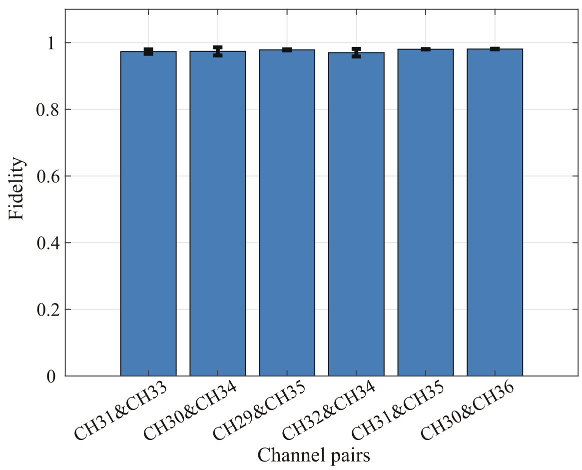

Fig. 4. The fidelity of polarization entanglement for each user-associated channel.

with a total transmission distance of 300 km of fiber (total transmission loss of 60 dB). To guarantee the security of the channel, the sequence of the emitted light from the two lasers can be regulated and the relevant information can be conveyed to the user via a classical channel. The user can then verify the security of the channel by comparing the precise position of the signal photon with that of the noise photon. Once the security of the network is guaranteed, the communication task can be initiated. It is essential that each user is equipped with a quantum memory to regulate the time of stored photons. We distribute the entangled photon pairs to the users, the sender performs a coding operation on the photons he gets and chooses specific basis vectors for the measurement. Subsequently, the sender tells the receiver the measurement results, and the receiver also chooses different basis vectors to measure the photons it gets. The receiver compares the two measurements to complete the Bell-state analysis and thus obtains the information transmitted by the sender. This conformity counting is done after transmitting a 300 km fiber optic distance, and the transmission of the measurement results is based on electrical signal transmission. In our experiment, we utilize a circuit delay module to regulate the electrical signals for time delay, with a time of stored photons that is considerably longer than the transmission time of 300 km (approximately 1.5 ms). The polarization Sagnac interferometer is modulated so that it produces photon pairs with an initial quantum state of $|\varphi^+\rangle_{\lambda_1(\lambda_2)}$, and the additional noise generator is then modulated before the distribution of the photon pairs, allowing for the introduction of modified noise. Then the photon pair is subsequently distributed to any two users U_A and U_B of the communication system. The fidelity $\langle \overline{F} \rangle$ of the entangled photons can be calculated from Eq. (1):

$$\langle \overline{F} \rangle = 1 - (p_A + p_B - 2p_A p_B). \tag{2}$$

Theoretically, varying p_A, p_B can bring the fidelity of the entangled photon pairs to 1, but in practice we are unable to do this due to dark counting in the detector and the drop in photon count due to transmission losses. The maximum fidelity that can actually be achieved is $F_{max} = (3V + 1)/4$, where V can be estimated in theory [50]. Considering that the transmission distance for distributing entangled photon pairs to different users and the transmission loss of C-band photons in optical fibers are basically the same, we assume that the total probability of inversion of two optical quantum bits, as well as the probabilities of each part, are equal, i.e., $p = p_A = p_B, p_{A,trans} = p_{B,trans}, p_{A,extra} = p_{B,extra}$. At different distances, we select a suitable noisy environment and measure the rate at which this network transmits a single type of bit 00 as shown in Fig. 5a. Limited by the fact that the single photon count of the SNSPD saturates at about 3×10^5–4×10^5 Hz, our network can only achieve a transmission rate of nearly 30,000 bits/s at 0 km. After 300 km of fiber optic transmission loss, the single photon counts of the SNSPD are only about 300–400 Hz left. To achieve the intended task, such as images or text, it may be necessary to use detectors with higher single-photon saturation thresholds to increase transmission rates. The variation of the fidelity of the entangled photon pairs with the transmission distance when different additional noises are introduced as shown in Fig. 5b. At a transmission distance of 300 km fiber, the fidelity of the entangled state with the addition of extra noise is improved compared to that without the addition of extra noise and agrees well with the experimental data. The double-pumped structure nearly doubles the number of photons in a single channel, which allows us to better regulate the extra noise factor p to improve the fidelity of the system after transmission. After modulating the extra noise and distributing the photon pairs over a transmission distance of 300 km, we can realize the encoding of four kinds of bits by applying different quantum gates to the photons to modulate the Bell states of the photon pairs. As shown in Fig. 6, the polarization entanglement fidelity of the four different messages received by each channel, obtained from experimental measurements under double-pumped conditions. The

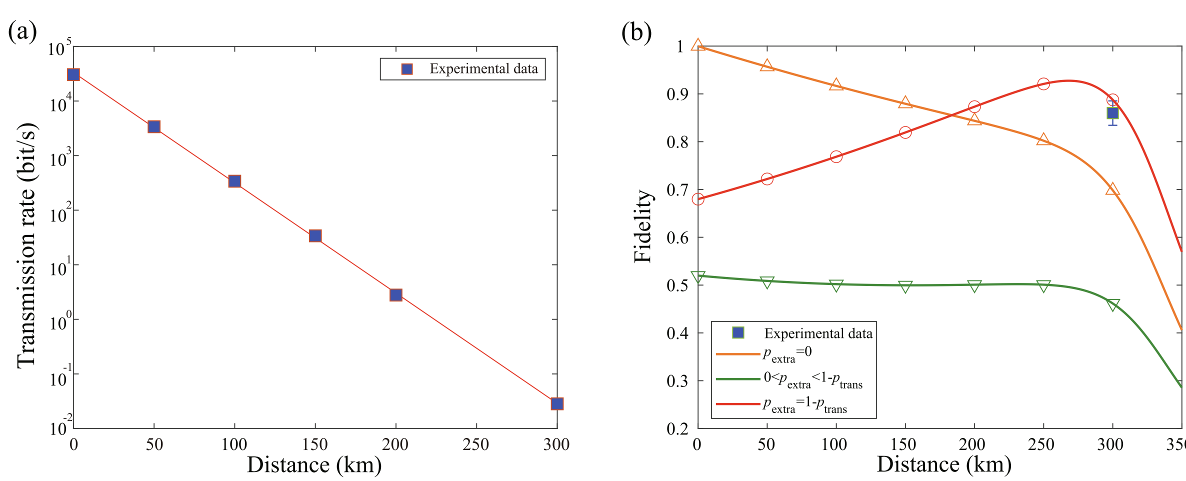

Fig. 5. (a) Transmission rate for transmitting a single kind of bit at different distances. (b) The variation of the fidelity of entangled photons with transmission distance for different levels of additional noise.

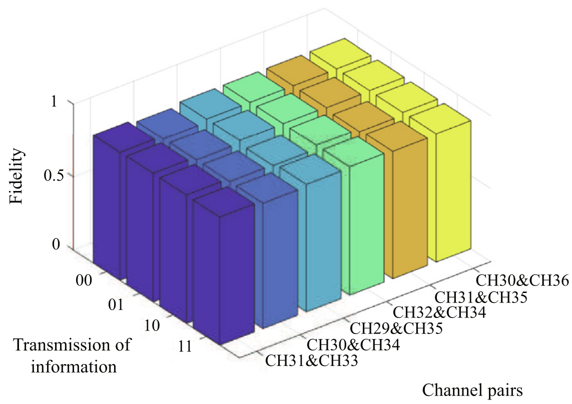

Fig. 6. The fidelity of polarization entanglement for four different coded messages after transmission.

measurement time for each data point is 10 min, and the fidelities are all in the range of 85%–87%, verifying the feasibility of this fully-connected network to realize QSDC over a distance of 300 km. Further improvement of the fidelity can be achieved by choosing a more efficient PPLN waveguide and applying a more matching extra noise.

The network we have designed is theoretically scalable. As the number of pumps increases, the number of channels required to distribute to individual users decreases. This allows for the accommodation of more users by adding more pumps when the number of channels is limited. From the measurement results of the typical spectrum of the SPDC source based on PPLNOI chip, it can be seen that near the C-band, this network can be used to construct a fully-connected quantum network with no less than 100 users (1500–1600 nm) using DWDM at 100 GHz, and the construction of a larger scale fully-connected quantum network can be extended based on the wavelength conversion technique [51]. Additionally, the incorporation of an appropriate noise environment can enhance the communication range of this network. When introducing noise, we solely consider the noise with the type of bit flip. However, incorporating other types of noise, such as phase flip noise and white noise, can further extend the transmission distance [41,52,53]. Furthermore, the use of noise can facilitate stealth communication, thereby enhancing the confidentiality of information transmission within the network [54]. These are all potential avenues for future exploration.

4. Conclusion

In conclusion, we have proposed a multipump expandable fully-connected QSDC network in noisy environments, which is designed to reduce its complexity and increase the number of users while guaranteeing communication distance between users. When the number of pumped light is two, an experimental realization of a four-user fully-connected QSDC network with 300 km fiber transmission is achieved. Each user in the network is found to only require the operation of two channels of photons to facilitate two-by-two communication. The results show that the fidelity of the shared entangled states between users by introducing additional noise reaches over 85% over a transmission distance of 300 km, and a QSDC of approximately 104 bits/h can be achieved. Our design of long-distance scalable fully-connected quantum network in noisy environments provides a novel idea for the construction of large-scale fully-connected quantum communication networks in the future.

Conflict of interest

The authors declare that they have no conflict of interest.

Acknowledgments

This work was supported in part by the National Natural Science Foundation of China (12074155, 62375164, and 12192252), the Shuguang Program of Shanghai Education Development Foundation and Shanghai Municipal Education Commission (24SG53), the Guangdong Provincial Quantum Science Strategic Initiative (GDZX2403003), the Foundation for Shanghai Municipal Science and Technology Major Project (2019SHZDZX01-ZX06), and SJTU (21X010200828).

Author contributions

Xianfeng Chen and Yuanhua Li conceived the idea of this paper. Yilin Yang and Yuanhua Li performed the simulations, drew all of the figures, and wrote the first draft based on the experiment's design and data. Chennan Wu, Hao Li, and Yuanlin Zheng provided experimental assistance. Xianfeng Chen supervised the overall project. All authors discussed the results and reviewed the manuscript.

References

[1] Vallone G, Gianani I, Inostroza E, et al. Testing hardy's nonlocality proof with genuine energy-time entanglement. Phys Rev A 2011;83:042105.
[2] Liao S, Cai W, Handsteiner J, et al. Satellite-relayed intercontinental quantum network. Phys Rev Lett 2018;120:030501.
[3] Joshi S, Aktas D, Wengerowsky S, et al. A trusted node–free eight-user metropolitan quantum communication network. Sci Adv 2020;6:eaba0959.
[4] Chen Y, Zhang Q, Chen T, et al. An integrated space-to-ground quantum communication network over 4,600 kilometres. Nature 2021;589:214–9.
[5] Pompili M, Hermans S, Baier S, et al. Realization of a multinode quantum network of remote solid-state qubits. Science 2021;372:259–64.
[6] Wengerowsky S, Joshi S, Steinlechner F, et al. An entanglement-based wavelength-multiplexed quantum communication network. Nature 2018;564:225–8.
[7] Wang S, Chen W, Yin Z, et al. Field and long-term demonstration of a wide area quantum key distribution network. Opt Exp 2014;22:21739–56.
[8] Lucamarini M, Yuan Z, Dynes J, et al. Overcoming the rate–distance limit of quantum key distribution without quantum repeaters. Nature 2018;557:400–3.
[9] Liu H, Jiang C, Zhu H, et al. Field test of twin-field quantum key distribution through sending-or-not-sending over 428 km. Phys Rev Lett 2021;126:250502.
[10] Li Y, Huang Y, Xiang T, et al. Multiuser time-energy entanglement swapping based on dense wavelength division multiplexed and sum-frequency generation. Phys Rev Lett 2019;123:250505.
[11] Sun Z, Cheng Y, Liu Y, et al. Message-oriented entanglement distribution network. IEEE Internet Things J 2024;11:35317–28.
[12] Cao Y, Zhao Y, Wang Q, et al. The evolution of quantum key distribution networks: on the road to the qinternet. IEEE Commun Surv Tutor 2022;24:839–94.
[13] Brunner H, Fung C, Peev M, et al. Demonstration of a switched CV-QKD network. EPJ Quantum Technol 2023;10:38.
[14] Shi S, Wang Y, Tian L, et al. Continuous variable quantum teleportation network. Laser Photonics Revs 2023;17:2200508.
[15] Wu Y, Tian L, Yao W, et al. Continuous variable quantum teleportation network with star topology. Appl Phys Lett 2024;124:114002.
[16] Long G, Pan D, Sheng Y, et al. An evolutionary pathway for the quantum internet relying on secure classical repeaters. IEEE Netw 2022;36:82–8.
[17] Wang M, Zhang W, Guo J, et al. Experimental demonstration of secure relay in quantum secure direct communication network. Entropy 2023;25:1548.
[18] Sun Q, Mao Y, Chen S, et al. Quantum teleportation with independent sources and prior entanglement distribution over a network. Nat Photonics 2016;10:671–5.
[19] Liuzzo-Scorpo P, Mari A, Giovannetti V, et al. Optimal continuous variable quantum teleportation with limited resources. Phys Rev Lett 2017;119:120503.
[20] Long G, Liu X. Theoretically efficient high-capacity quantum-key-distribution scheme. Phys Rev A 2002;65:032302.
[21] Li T, Long G. Quantum secure direct communication based on single-photon bell-state measurement. New J Phys 2020;22:063017.

[22] Liu X, Li Z, Luo D, et al. Practical decoy-state quantum secure direct communication. Sci China Phys Mech Astron 2021;64:120311.
[23] Ying J, Zhao P, Zhong W, et al. Passive decoy-state quantum secure direct communication with a heralded single-photon source. Phys Rev Appl 2024;22:024040.
[24] Zhao P, Zhong W, Du M, et al. Quantum secure direct communication with hybrid entanglement. Front Phys 2024;19:51201.
[25] Sun Z, Song L, Huang Q, et al. Toward practical quantum secure direct communication: a quantum-memory-free protocol and code design. IEEE Trans Commun 2020;68:5778–92.
[26] Pan D, Lin Z, Wu J, et al. Experimental free-space quantum secure direct communication and its security analysis. Photonics Res 2020;8:1522–31.
[27] Liu X, Luo D, Lin G, et al. Fiber-based quantum secure direct communication without active polarization compensation. Sci China Phys Mech Astron 2022;65:120311.
[28] Cao Z, Lu Y, Chai G, et al. Realization of quantum secure direct communication with continuous variable. Research 2023;6:0193.
[29] Paparelle I, Mousavi F, Scazza F, et al. Practical quantum secure direct communication with squeezed states, arXiv preprint arXiv:2306.14322; 2023.
[30] Sheng Y, Zhou L, Long G. One-step quantum secure direct communication. Sci Bull 2022;67:367–74.
[31] Zhou L, Sheng Y. One-step device-independent quantum secure direct communication. Sci China Phys Mech Astron 2022;65:250311.
[32] Zhou L, Xu B, Zhong W, et al. Device-independent quantum secure direct communication with single-photon sources. Phys Rev Appl 2023;19:014036.
[33] Zeng H, Du M, Zhong W, et al. High-capacity device-independent quantum secure direct communication based on hyper-encoding. Fundam Res 2024;4:851–7.
[34] Zhou Z, Sheng Y, Niu P, et al. Measurement-device-independent quantum secure direct communication. Sci China Phys Mech Astron 2020;63:230362.
[35] Ying J, Zhou L, Zhong W, et al. Measurement-device-independent one-step quantum secure direct communication. Chin Phys B 2022;31:120303.
[36] Cao Z, Wang L, Liang K, et al. Continuous-variable quantum secure direct communication based on gaussian mapping. Phys Rev Appl 2021;16:024012.
[37] Yang L, Wu J, Lin Z, et al. Quantum secure direct communication with entanglement source and single-photon measurement. Sci China Phys Mech Astron 2020;63:110311.
[38] Zhu F, Zhang W, Sheng Y, et al. Experimental long-distance quantum secure direct communication. Sci Bull 2017;62:1519–24.
[39] Zhang H, Sun Z, Qi R, et al. Realization of quantum secure direct communication over 100 km fiber with time-bin and phase quantum states. Light Sci Appl 2022;11:83.
[40] Qi Z, Li Y, Huang Y, et al. A 15-user quantum secure direct communication network. Light Sci Appl 2021;10:183.
[41] Pan D, Long G, Yin L, et al. The evolution of quantum secure direct communication: on the road to the qinternet. IEEE Commun Surv & Tutor 2024:1898–949.
[42] Fortes R, Rigolin G. Fighting noise with noise in realistic quantum teleportation. Phys Rev A 2015;92:012338.
[43] Knoll L, Schmiegelow C, Larotonda M. Noisy quantum teleportation: an experimental study on the influence of local environments. Phys Rev A 2014;90:042332.
[44] Fortes R, Rigolin G. Probabilistic quantum teleportation in the presence of noise. Phys Rev A 2026;93:062330.
[45] Deng F, Long G, Liu X. Two-step quantum direct communication protocol using the einstein-podolsky-rosen pair block. Phys Rev A 2003;68:042317.
[46] Ortega E, Dovzhik K, Fuenzalida J, et al. Experimental space-division multiplexed polarization-entanglement distribution through 12 paths of a multicore fiber. PRX Quantum 2021;2:040356.
[47] Huang C, Hu X, Liu B, et al. Experimental one-step deterministic polarization entanglement purification. Sci Bull 2022;67:593–7.
[48] Ecker S, Sohr P, Bulla L, et al. Remotely establishing polarization entanglement over noisy polarization channels. Phys Rev Appl 2022;17:034009.
[49] Mattle K, Weinfurter H, Kwiat P, et al. Dense coding in experimental quantum communication. Phys Rev Lett 1996;76:4656.
[50] Wu J, Huang Y, Lu C, et al. Tunable linear polarization-state generator of single photons on a lithium niobate chip. Phys Rev Appl 2020;13:064068.
[51] Joshi C, Farsi A, Clemmen S, et al. Frequency multiplexing for quasi-deterministic heralded single-photon sources. Nat Commun 2018;9:847.
[52] Caruso F, Huelga S, Plenio M. Noise-enhanced classical and quantum capacities in communication networks. Phys Rev Lett 2010;105:190501.
[53] Fonseca A. High-dimensional quantum teleportation under noisy environments. Phys Rev A 2019;100:062311.
[54] Liu Y, Arrazola J, Liu W, et al. Experimental covert communication over metropolitan fibre optical links. IEEE Wirel Commun 2024;31:76–80.